PHYSICAL REVIEW B VOLUME 5, NUMBER 10 15 MAY 1972

Renormalized Atoms and the Band Theory of Transition Metals

L. Hodges
Institute for Atomic Research and Department of Physics, Iowa State University, Ames, Iowa* 50010
and
R. E. Watson
Brookhaven National Laboratory, Upton, New York* 11973
and
H. Ehrenreich†
Division of Engineering and Applied Physics, Harvard University, Cambridge, Massachusetts 02138
(Received 2 November 1971)

The renormalized-atom approach, first used by Chodorow, is shown to yield quantitative estimates of some of the essential potential-dependent parameters characterizing transition-metal band structures on the basis of essentially atomic considerations. These are the position Γ_1 of the conduction-band minimum, the mean d-band energy, the energies associated with d-band extrema, and the degree of s-d hybridization as defined within the Heine-Hubbard pseudopotential schemes. The estimates of Γ_1 and the d-band extrema utilize "renormalized-atom" band potentials within the Wigner-Seitz cell in which the interelectronic exchange is taken into account without resort to the $\rho^{1/3}$ approximation and incorporate the appropriate boundary conditions at the Wigner-Seitz radius r_{WS}. The results have comparable accuracy with those obtained from augmented-plane-wave calculations employing the same crystal potential within the muffin-tin approximation. The band results are qualitatively similar to those obtained using more conventional $\rho^{1/3}$ potentials. The Wigner-Seitz viewpoint is thereby seen to be useful in obtaining quantitative results for certain high-symmetry points in k space aside from Γ_1 with far less computational effort. In addition, the present scheme may provide a better starting point for dealing with d-d exchange-correlation effects. Also discussed are a number of features general to the problem of constructing adequate transition-metal crystal potentials, in particular, how to deal with nonintegral d- and conduction-electron counts per atom, and configuration and/or multiplet averaging.

I. INTRODUCTION

While energy-band calculations in transition and noble metals have been successful in reproducing such complicated experimental data as Fermi surfaces, there is no over-all satisfying explanation of their electronic and magnetic properties at the present time. The complication, of course, arises from the presence of two distinct species of band electrons arising, respectively, from the d and conduction bands. The conduction-electron properties are presumably similar to those encountered in "simple" metals, such as K and Al, and experience[1] with exchange and correlation effects in such metals may be useful here. Because of their tight-binding-like character, it is less obvious that this same experience has much relevance to d electrons. Here intra-atomic exchange and correlation effects of the sort considered by Van Vleck,[2] Hubbard,[3] and Gutzwiller[4] may be of considerable importance.

This paper will consider a class of band potentials[5] which may provide a useful starting point for the incorporation of intra-atomic d-d exchange and correlation effects in potentials appropriate to the transition metals. Such considerations will be of importance in the explanation of the cohesive energy of pure metals as well as the single-electron properties of alloys having these as constituents. These potentials will be used to investigate the potential-dependent parameters involved in the orthogonalized plane-wave (OPW)–tight-binding–Korringa-Kohn-Rostoker (KKR)–pseudopotential schemes developed by Heine,[6] Hubbard,[7] and others.[8] (With apologies to other workers, this approach will be termed the Heine-Hubbard theory.) The renormalized-atom picture[5] will be described in detail and shown to yield the structure-independent properties of the bands satisfactorily.

The renormalized-atom approach was first used by Chodorow,[9] and extended by Segall[10] for Cu. In this scheme one utilizes the free-atom s and d wave functions, truncates them at the radius r_{WS} of the Wigner-Seitz (WS) sphere, and renormalizes them within this sphere, thereby preserving charge neutrality. This procedure preserves the shape of the wave functions inside the sphere. In this way the atoms are "prepared" in approximately the form in which they actually enter the solid before placing them together. By beginning with renormalized wave functions rather than free-atom charge den-

sities in constructing a potential, interelectronic exchange may be explicitly introduced and correlation effects taken into account to the same extent as in the Wigner-Seitz method. In this method a full self-Coulomb hole is supposed attached to the site at which the electron is sampling the potential. The result is thus not identical to a Hartree-Fock derivation of a band potential. The procedure, which is in closer parallel to that followed in atomic calculations, obviates the necessity of using local-density-dependent $\rho^{1/3}$ potentials of either the Slater[11] or Gaspar-Kohn-Sham form.[12] The use of a local-density-dependent potential then becomes a matter of physical choice rather than computational necessity. One might, for example, choose to apply the $\rho^{1/3}$ approximation to the transition-metal conduction bands. Unlike the local-density approximation, the renormalized-atom approach introduces a correlation hole centered in the Wigner-Seitz cell. This could be a poor approximation for an itinerant electron sampling the outer portions of a Wigner-Seitz cell where a correlation hole might be more appropriately centered about the electron's position. The $\rho^{1/3}$ or some other approximation might be better here. The situation is different for d electrons. Most important to their properties is the potential in the interior of the ion, in the region indicated in Fig. 1. In this case, the renormalized-atom approach seems an excellent first approximation. The d-d exchange-correlation problem then centers on how one modifies the Wigner-Seitz approximation. The previous work of Van Vleck and of Hubbard provides substantial physical guidelines as to how this might be accomplished.

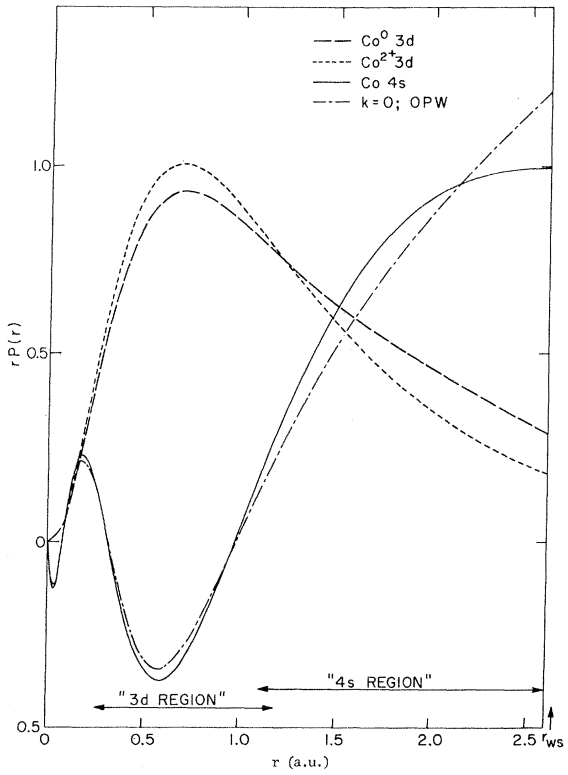

FIG. 1. Co $3d$ and $4s$ radial functions $rP(r)$ obtained by renormalizing free-atom $3d^8 4s^2$ and $3d^{10}$ functions to the Wigner-Seitz sphere. Also shown is a $k=0$ orthogonalized plane wave, similarly normalized to the Wigner-Seitz sphere.

l-dependent Hartree-Fock–Wigner-Seitz potentials, henceforth termed "renormalized-atom potentials" for both d and conduction bands, will be explored in this paper. Questions of self-consistency will not be considered, but deferred to a subsequent paper. Even so, the band results will be seen to be in reasonable accord with experience based on experiment and on calculations employing other types of potentials.

Of equal importance in this paper will be the investigation of the potential-dependent parameters important to a transition-metal band structure. While the renormalized-atom scheme is useful in such a study, it is in fact unimportant as to whether the band potential itself is or is not of the renormalized-atom type. The parameters of interest are the following: (i) the energy location ϵ_Γ of Γ_1, the bottom of the conduction band relative to the constant muffin-tin potential between augmented-plane-wave (APW) spheres, (ii) the location ϵ_d of the resonant d level at each atomic site, which will be shown to define the mean d-band position, and (iii) the d-band widths and the parameter determining the degree of d hybridization with the conduction bands. The renormalized-atom approach will be shown to have considerable utility in that essentially atomic estimates can provide a good representation of these parameters. In this context, the simple Wigner-Seitz boundary conditions, normally applied to conduction bands, will be seen to be more important to d-band properties than is generally recognized.

The renormalized-atom concept is useful, in addition, in permitting easier visualization of the sources of the cohesive energy[13] and compressibility of transition metals which are still not completely understood. Another application, which in fact is the original motivation for this work, is in connection with nondilute ordered and disordered alloys. The renormalized-atom scheme is useful both in constructing potentials of such systems and as a means for understanding[14] the chemical shifts of core and valence levels. The scheme may also be exploited in estimates of the screening of the Coulomb repulsion term appearing in the Hubbard Hamiltonian.[3] These matters are not considered in the present paper.

Section II defines and discusses the renormalized-atom scheme. Among the matters considered here are (a) the magnitude of the absolute shift of ϵ_d, relative to the free-ion d energy, upon renormalization, (b) the construction of l-dependent renormalized-atom potentials appropriate to the method, and (c) approaches that may be useful in constructing potentials that take into account the fact that transition metals frequently have nonintegral numbers of d and conduction electrons per atom.

Several points of detail, important to the calculations, are discussed in appendices. Appendix A deals with the properties of intra-atomic exchange and the problems associated with its utilization in band calculations. Appendix B presents some details of the calculations. Having restricted the self-Coulomb hole to the WS cell within which the potential is defined, the metal outside the cell is neutrally charged, but it nevertheless may make multipole contributions to the zero of the spherical potential inside. These are estimated in Appendix C and are found to be insignificantly small, as might be expected.

Renormalized-atom potentials of the type discussed in Sec. II are used throughout the remainder of the paper. The band results arising from this choice are of interest in themselves but the observations which will be made concerning the relation of the potential-dependent band parameters deduced from the renormalized-atom viewpoint and the results of band calculations are quite independent of the choice of the potential. This viewpoint therefore permits simple and reliable estimates of some of the most important parameters determining a transition-metal band structure which can only be obtained with a great deal of effort using the muffin-tin approaches to band theory. In short, it resurrects a point that seems to have been lost sight of in recent years: that the Wigner-Seitz viewpoint is both simple and as accurate as standard band calculations when applied to structure-independent features of the bands at high-symmetry points.

These points are illustrated in Secs. III and IV. The former is concerned with the placement of ϵ_d and ϵ_Γ. Atomic estimates of the energy of a renormalized d function in the d-band potential associated with a single WS cell accurately predict the mean ϵ_d, corresponding to the center of gravity of the d bands obtained from APW calculations employing the same crystal potential in the muffin-tin approximation. Similar atomic estimates yield ϵ_Γ equally accurately. It should be emphasized, however, that the d functions utilized above are free-atom functions truncated at and renormalized to the WS cell. By contrast the s functions determining ϵ_Γ are obtained in the standard Wigner-Seitz manner by integrating the Schrödinger equation in the renormalized potential and installing the boundary condition that it have zero slope at the Wigner-Seitz radius r_{WS}.

Section IV deals with other features of transition-metal band structures that may be deduced from the renormalized-atom approach. One of these is the width of the unhybridized d bands. The d-band extrema obtained by finding energies corresponding to d functions, $P(r)$, satisfying Wigner-Seitz conditions at r_{WS} (and not at r_{APW} as in Heine's work) appropriate to "bonding" ($dP/dr_{WS}=0$) and "antibonding" [$P(r_{WS})=0$] orbitals are in excellent agreement with the d-band extrema resulting from APW or KKR calculations. The $P(r)$ in question are obtained by integrating the Hartree-Fock equation containing the renormalized-atom d potential over the full Wigner-Seitz cell, without recourse to the muffin-tin approximation. In this connection, it will be noted that the $P(r)$ obtained in this way are nearly identical to those found from band calculations. Accordingly, in addition to accurate estimates of the more important energies, the renormalized-atom approach also yields proper wave functions which are defined over the full Wigner-Seitz sphere.

The strength of the s-d hybridization is also discussed, albeit briefly, since the present results are in essential agreement with those of Heine.

The Wigner-Seitz approximation is known[15] to provide excellent estimates of ϵ_Γ. Thus the agreement with APW theory that is found here is not surprising. The more novel aspect of the present work is that the same atomic considerations can be applied equally successfully to the energies characterizing the mean (ϵ_d) and the extrema of the d bands as well as the corresponding eigenfunctions.

II. RENORMALIZED ATOMS

The renormalized-atom approach permits the definition of a wave function rather than a charge density throughout the Wigner-Seitz sphere and preserves the shape of the atomic wave function in the interior of the ion core. Interelectronic exchange terms may then be derived. This cannot be done with the charge density resulting from the standard energy-band practice of superimposing free-atom charge densities. The superposition may be said to violate the Pauli exclusion principle in that it does not preserve proper wave-function shape in the interior of the ion. The implications of this are most serious for transition metals where the potential in this region is important to d-band properties. Renormalized $3d$ and $4s$ functions for various atomic configurations of Co are shown in Fig. 1. The quantity $rP(r)$, whose square is the charge density at radius r, shown there is such that the normalization condition

$$\int_0^{r_{WS}} [rP(r)]^2 dr = 1 \tag{1}$$

is maintained. The radial regions where the details of the potential are most important to the $3d$- and $4s$-electron behavior are also indicated. Thus, in the $3d$ region the detailed behavior of the potential dominates in determining the d-electron energy and the shape of the wave function at some given energy. While the charge outside this region affects ϵ_d, its primary influence is to produce a potential well in which the $3d$ electrons are placed. The gross features of this charge density, such as the requirement that a Wigner-Seitz cell be neutrally charged, rather than its precise shape are of predominant significance. The importance of the inner region is in large part due to the centrifugal barrier arising from the angular kinetic energy. The $4s$ electrons with their larger principal quantum number are more diffuse and therefore the potential at larger distances from the nucleus becomes important. The same trend occurs in the $4d$ and $5d$ metals. Here too the d electrons sample regions inside those important to conduction electrons.

The importance of the inner region to d potentials provides incentive to exploit the renormalized-atom approach and to implement quantitatively the views of Van Vleck and Hubbard which emphasize intra-atomic exchange and correlation.

A. Wave Functions and Energy Shifts

Let

$$\phi_j(\vec{r}) \equiv \begin{cases} N\tilde{\phi}_j(\vec{r}), & r \le r_{WS} \\ 0, & r > r_{WS} \end{cases} \tag{2}$$

be the renormalized wave function, the radial part being P. Here $\tilde{\phi}_j$ is a free-atom function cut off at r_{WS} and N is a constant normalizing it to the Wigner-Seitz sphere. Figure 1 shows examples of the radial parts of such free-atom renormalized wave functions for Co.

The differences in the d function shown in Fig. 1 are characteristic of, though smaller than, the variation in d character actually encountered in a set of d bands (an example, for Co, is discussed in connection with Fig. 11). Note that the shape of the functions is essentially the same in most of the "$3d$ region." This fact is important to the derivation of a common exchange potential which can be usefully applied to d states anywhere in the bands. This matter is considered in Appendix A. The ϕ_j defined in Eq. (2) may be used to construct the renormalized-atom potential $V_i^\alpha(r)$ within the Hartree localized exchange approximation[16] in the following manner:

$$V_i^\alpha(r)\,\phi_i^\alpha(r) \equiv \left(\sum_{j\{\alpha\}} \int_{WS} |\phi_j^\alpha(r')|^2 \frac{2}{|\vec{r}-\vec{r}|} d^3r' - \sum_{j\{\alpha\}} \delta(m_{si}, m_{sj}) \frac{\phi_j^\alpha(r)}{\phi_j^\alpha(r)} \int_{WS} \phi_j^{\alpha *}(r')\,\phi_i^\alpha(r') \frac{2}{|\vec{r}-\vec{r}'|} d^3r' - \frac{2Z}{r} \right) \phi_i^\alpha(r) \tag{3}$$

(atomic-rydberg units are used throughout). The superscript α on ϕ_j denotes the atomic configuration and the sum over j spans the ion core plus the occupied valence-electron states. The energy of a d electron in a potential V_i^α is approximately

$$\epsilon_d \equiv \epsilon_d^{\text{ren}} = \langle \phi_d^\alpha(r) | \nabla^2 + V_d^\alpha(r) | \phi_d^\alpha(r) \rangle . \tag{4}$$

This estimate will be seen to be in excellent numerical agreement with the band pseudopotential parameter which marks the center of gravity of the d bands obtained from V_d. This result is attractive in view of its immediate physical interpretability but may seem surprising since ϕ_d is, in general, somewhat different spatially than either the band wave function at ϵ_d or some average band function. The success of Eq. (4) follows from the infrequently exploited fact that, given V_d, ϵ_d is actually insensitive to the details of ϕ_d. This insensitivity results from a competition between the potential and the $l(l+1)/r^2$ centrifugal term in the "d region." This feature is absent in the case of conduction electrons.

One reason why the renormalized-atom ϕ_d are a reasonable first approximation to the metal (and are useful in predicting ϵ_d) is that d renormalization is not too severe. This is seen in the bottom of Fig. 2 for the $d^{n-1}s^1$ configuration. The *free-atom* d charge lying outside r_{WS} ranges from about 2% in Ag to slightly in excess of 20% for Y. The percentages are smaller in the $d^{n-2}s^2$ and larger in the $d^n s^0$ configurations, but in all cases they are small compared with the 60–75% effects associated with the valence s electrons shown in the upper section of the figure. The Heine-Hubbard type of approach to the transition metals assumes, in a variety of ways, that there is little d charge in the outer parts of the WS cell. One might therefore expect this approach to be inapplicable to the case of metals like Y. Nevertheless, it will be shown here that the renormalized-atom approach to the Heine-Hubbard theory yields results for Y that are of comparable accuracy as those for Co or Cu.

With two-thirds to three-quarters of their free-

atom charge outside r_{WS}, the valence s electrons undergo a substantial compression on going into the metal. Such a compression is also a characteristic of the simple metals, such as K, and it is important to their cohesion. In the free atom, the valence electron lies outside an attractive +1-charged ion core and it would contract if it were not for the cost in increased kinetic energy. Because the outside boundary conditions of a free atom and one embedded in a solid are different, the contraction can be achieved in the solid with a net lowering of the energy. The wave function at the bottom of the conduction band ($k = 0$) meets the Wigner-Seitz boundary condition since it is flat at r_{WS}. An example is shown in Fig. 1. Since $rP(r)$ and not $P(r)$ is plotted, the function is proportional to r in the outer portion of the cell. Its energy ϵ_Γ is lower than that of either the free-atom or the renormalized-atom s function. The latter, which is also shown in this figure, has greater curvature in the "4s region" and as a result an increased kinetic energy. The associated energy is ~ 0.4 Ry higher than ϵ_Γ. Simple calculations in the spirit of Wigner-Seitz would place the origin of a free-electron parabola at ϵ_Γ and fill the band to the level necessary to accommodate the required number of electrons. These yield estimates

$$\delta E = \epsilon_\Gamma + \tfrac{3}{5}k_F^2 - \epsilon_{at} \qquad (5)$$

of the cohesive energy for, say, K which are within 97% of the observed value. The same effect is important to the cohesion in the transition metals,[12]

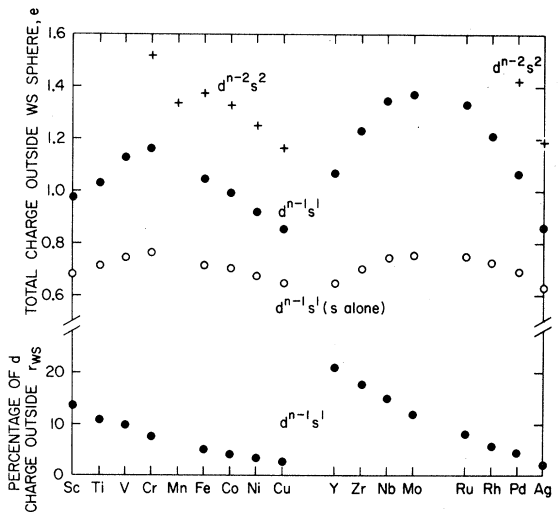

FIG. 2. Percentage of free-$d^{n-1}s$-atom d charge lying outside the metal Wigner-Seitz spheres (bottom plot); also, the s and total s-plus-d free-$d^{n-1}s$-atom charge which lies outside r_{WS} (top plots). Limited data are shown for the total exterior charge associated with the $d^{n-2}s^2$ free-atom configuration.

although the considerations are considerably complicated by the presence of the d electrons in these materials. In solids it is ϵ_Γ rather than some center of gravity of the conduction bands that is of primary importance, and accordingly its behavior will be monitored in the discussions to follow.

The total free-atom charge outside r_{WS} provides the best measure of the full renormalization effect. Data for the $d^{n-1}s^1$, and some for the $d^{n-2}s^2$, configurations are plotted at the top of Fig. 2. The rise, going from Cu or Ag to the left across a row, is largely due to an increase in free-ion size while r_{WS} holds almost constant. The experimental r_{WS} increase substantially to the left of Cr and Mo and this, plus the dropping d-electron count, overpower any increasing ion size, causing the dropoff in the curves. The relation of r_{WS} to ion size is important to the cohesion of the transition metals. This matter will be discussed elsewhere. Of immediate consequence to the present paper is the effect of renormalization on the band structure.

The results of Fig. 2 for the total charge show that roughly one electron's worth of charge which lies outside r_{WS} in the free atoms must be brought inside the Wigner-Seitz sphere in a metal in order to ensure charge neutrality within the unit cell. It should be recognized that this charge shift will occur in these monatomic metals even if the potential is constructed by the more conventional means of overlapping atomic charges. In ordered binary alloys, the atomic cell of some atomic species will not be necessarily neutral. The required charge shift between constituents can be easily incorporated by constructing a potential of the renormalized-atom variety in which each atomic cell is initially neutral or suitably charged. By contrast, the standard superposition of free-atom charge densities treats this charging effect in an uncontrolled manner, unless the calculations are carried through to self-consistency.

In order to obtain some physical feeling for the magnitude of the d-level shift resulting from renormalization, it may be useful at the outset to estimate crudely the effect of the leading term which is the compression of s charge,

$$q \equiv \int_{r>r_{WS}} \rho_{at}(r)\, d^3r\,, \qquad (6)$$

originally outside r_{WS} into the WS sphere. Here $\rho_{at}(r)$ is the s charge density corresponding to the free atom. As this charge is shifted inside r_{WS}, it produces a repulsive Coulomb contribution Δ to the d-electron potential. If, for simplicity, it is assumed that the d electrons lie in the inner region of the atom in which $\rho_{at}(r)$ is small, then Δ may be written as the difference of two Coulomb energies:

$$\Delta = 2q(R_{ren}^{-1} - R_{at}^{-1})\,. \qquad (7)$$

Here

$$R_{\rm at}^{-1} \equiv q^{-1} \int_{r>r_{\rm WS}} \rho_{\rm at}(r)\, r^{-1}\, d^3 r \tag{8}$$

is the average inverse radial distance associated with the charge in the free atom to be shifted and

$$R_{\rm ren}^{-1} \equiv q^{-1} \int_{r<r_{\rm WS}} [\rho_{\rm ren}(r) - \rho_{\rm at}(r)]\, r^{-1}\, d^3 r$$

$$= \frac{\int_{r<r_{\rm WS}} \rho_{\rm at}(r)\, r^{-1}\, d^3 r}{\int_{r<r_{\rm WS}} \rho_{\rm at}(r) d^3 r} \tag{9}$$

is that associated with the charge q after it has been shifted in accord with the renormalization prescription for which $\rho_{\rm ren}(r) = C\rho_{\rm at}(r)$, C being a constant and $r \leq r_{\rm WS}$. For Co (d^8s) one finds $R_{\rm ren}^{-1} = 0.60$ a.u., $R_{\rm at}^{-1} = 0.26$ a.u., and $q = 0.7$, which results in $\Delta = 0.5$ Ry, which may seem surprisingly large. The radial distances satisfy the expected inequality $R_{\rm ren} < r_{\rm WS} < R_{\rm at}$. Since $r_{\rm WS}$ and q vary relatively slowly over all but the lightest elements of the $3d$ row, one can expect this result to be characteristic for most of its members in the $d^n s$ configuration. This expectation will be confirmed below; ϵ_d lies substantially above the free-atom one-electron energy $\epsilon_d^{\rm at}$. For the $d^{n-1}s$ configuration the total d shift results from about equal Coulomb contributions from d-d and d-s interactions. The d-d contribution is large despite the small renormalization effects experienced by the d electrons because there are many of them per atom.

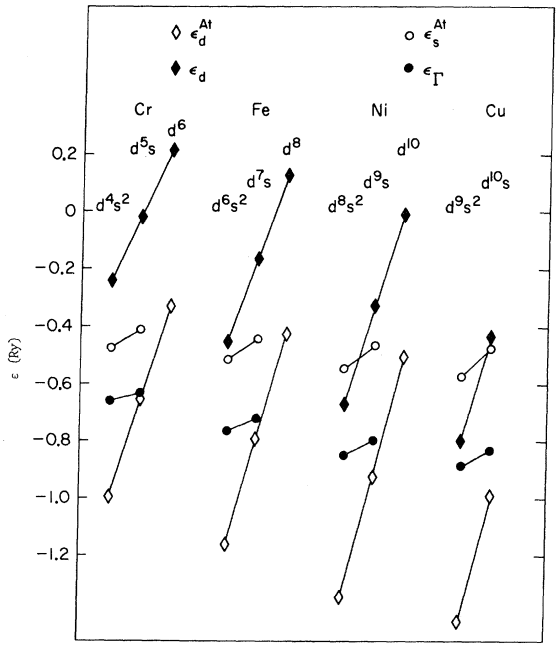

FIG. 3. Free-atom ($\epsilon_d^{\rm at}$ and $\epsilon_s^{\rm at}$) and renormalized-atom (ϵ_d and ϵ_Γ) one-electron energies for Cr, Fe, Ni, and Cu in the d^n, $d^{n-1}s$, and $d^{n-2}s^2$ configurations. ϵ_Γ was obtained for a $k = 0$ orthogonalized plane wave in the renormalized-atom Hartree-Fock potential. ϵ_d was obtained for the renormalized d function of the atomic configuration in question.

An estimate of $\epsilon_d - \epsilon_d^{\rm at}$ based on Eq. (4) accounts for the renormalization change of both the full potential and the d function and is therefore expected to be more reliable. d-level shifts for a few $3d$ elements are shown in Fig. 3. A more complete survey of results for the $3d^{n-1}s$ configuration will be considered in Sec. III. However, the present results are characteristic. Here the d levels are shifted upward by 0.5–0.75 Ry, with respect to vacuum, while the s-band origin ϵ_Γ is lower than the free-atom s energy for reasons discussed earlier. The d shifts are seen to be greatest for the $d^{n-2}s^2$ and least for the d^n configuration.

It has been frequently assumed in the literature that the resonant d level, marking the center of gravity of the d bands, is at or close to its free-atom value. The results above indicate that this assumption is seriously in error.

The large upward shift of the d levels upon renormalization may seem surprising since one might naively suppose that this is accompanied by a corresponding increase in the total Hartree-Fock energy of the renormalized atom. In fact, as has been indicated previously,[5,13] the total Hartree-Fock energy varies very little with renormalization. This is because the two-electron Coulomb (U_{ij}) and exchange (J_{ij}) terms which are responsible for the renormalization shifts must not be double counted in the total energy; i.e., the single-electron energy terms which must be summed to give the total are

$$\epsilon_i - \tfrac{1}{2}\textstyle\sum_j [U_{ij} - J_{ij}\, \delta(m_{si}, m_{sj})]\,,$$

where the sum is over occupied states. Volume renormalization of the Coulomb terms in this equation virtually cancels the shifts associated with ϵ_d. The fact that the center of gravity of the d bands corresponds closely to the renormalized ϵ_d is nevertheless of considerable importance to questions of cohesion,[13] work functions, and to alloying properties.

The preceding discussion of the renormalized-atom approach to band theory is summarized in Fig. 4, in which Cu and Ni are chosen as examples. One starts with a free atom having a configuration which is as close as possible to that encountered in a solid. The renormalization procedure then yields the energies ϵ_d and ϵ_Γ, which correspond closely to the center of gravity of the d band and the bottom of the conduction band, respectively. The prepared atoms are then placed together. The d band broadens about ϵ_d and hybridizes with the conduction band, whose minimum still lies at ϵ_Γ.

This scheme is attractive because of its immediate physical interpretability and because it is easily implemented in certain more complicated metals containing several constituents. Furthermore, as has already been pointed out, exchange effects can be included in a more quantitative fashion, as can correlation effects, in terms of the pictures proposed by Van Vleck and Hubbard.

B. Potentials

Equation (3) describes a potential where, much as in a free atom, there is a full self-Coulomb hole attached to the Wigner-Seitz sphere in question. Atomic potentials of course involve configurations having an integral number of d and non-d electrons. However, it is characteristic of real transition metals that the number of such electrons may well be nonintegral. The possibility of the existence of nonintegral d counts will be included here by considering atoms having a $d^{n-x}s^x$ configuration in which x is not necessarily integral. In such an atom, the spherical Coulomb terms sampled, respectively, by a d and an s electron are

$$V_d(r) = (n-x-1)\chi_d(r) + x\chi_s(r) \tag{10a}$$

and

$$V_s(r) = (n-x)\chi_d(r) + (x-1)\chi_s(r)\,, \tag{10b}$$

where

$$\chi_i(r) \equiv \frac{2}{r}\int_0^r P_i^2(r')r'^2dr' + \int_r^\infty P_i^2(r')\frac{2}{r'}r'^2dr'\,. \tag{11}$$

The resulting potential constructed in this way is clearly l dependent. The utilization of such a potential in the present APW band calculations is discussed in Appendix B.

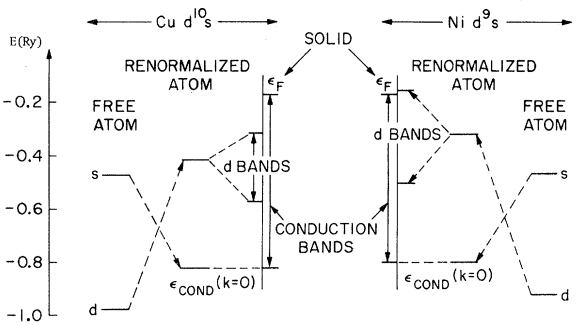

FIG. 4. Summary of renormalization and band contributions to the energy levels encountered in a transition metal as obtained for Cu and Ni in their $d^{n-1}s$ configurations. The energy of a $k=0$ orthogonalized plane wave, in the renormalized-atom s potential, is used to place the bottom of the conduction bands.

Interelectronic exchange contributions are accounted for using averages over given configurations. The "average-of-configuration" scheme[17] involves averaging the direct and exchange contributions over the full set of multiplet states which can be constructed from the $d^{n-x}s^x$ configuration in question. Potentials of this type have been widely employed in band calculations appropriate to nonmagnetic metals, but with approximations for the exchange terms which are not necessary here. Inclusion of exchange leads to equations having the same structure as Eqs. (10). However, the χ_i now include interaction terms corresponding to the exchange integrals. Potentials of this kind suffer from the fact that the interelectronic terms giving rise to Hund's rules in free atoms have been averaged out. This might be expected to be a serious shortcoming for magnetic metals such as Cr and Fe. In order to explore this approximation a few potentials will be considered where the average-of-configuration d-d terms have been replaced by counterparts characteristic of Hund's-rule ground multiplets. This replacement will be seen to have substantial effects on the resulting band structures. These examples will therefore serve to emphasize the importance of improving the d-d exchange-correlation potential to be used in band calculations.

C. Fractional Occupancy

The treatment of fractional occupancy which arises when the number of d and s electrons in the renormalized atom is nonintegral is not entirely straightforward and therefore deserves some further comment. There are two approaches which suggest themselves. One might choose to deal with a single atomic configuration of nonintegral count in, say, the average-of-configuration scheme[18] discussed above, or one might follow Van Vleck[2] and describe the atom as fluctuating between configurations of differing integral counts. This choice can be important to the treatment of d-d exchange-correlation effects for the resulting effective potentials to be used in a band calculation will differ for the two cases as will the estimates of interelectronic contributions to the cohesive energy.

The possible differences between the two choices becomes quite apparent when the number of one of the valence-electron species falls below one per atom, that is, when, in the present $d^{n-x}s^x$ notation, x is less than 1. Considering only spherical Coulomb terms, one obtains[19] from Eq. (10b) a *negative* s-s Coulomb contribution to the s potential of weight $x-1$. This is compensated by a d Coulomb contribution involving a charge greater than $n-1$. In the second multiconfiguration approach one might use a wave function having the form

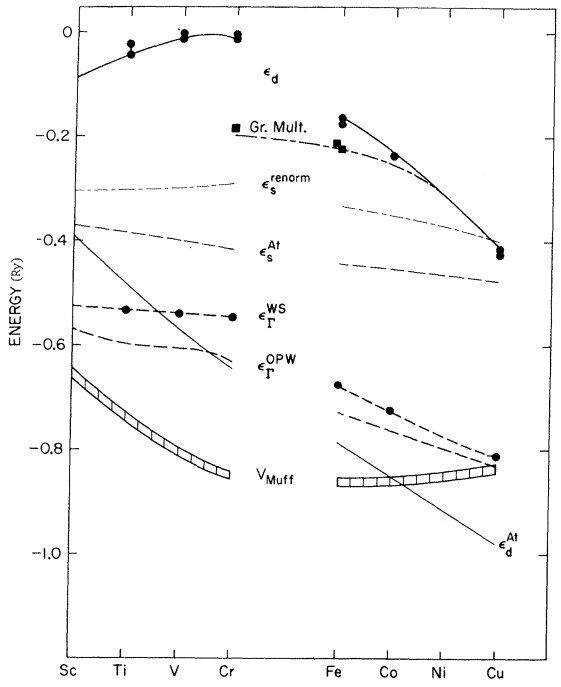

FIG. 5. Free- and renormalized-atom d (solid line) and s (dashed line) one-electron energies for the $3d^{n-1}4s^1$ metals. The points overlying the ϵ_d are d-band centers of gravity [e.g., $\frac{2}{5}\epsilon(\Gamma_{12}) + \frac{3}{5}\epsilon(\Gamma'_{25})$] obtained from APW band calculations based on the renormalized-atom potentials. The ϵ_Γ were obtained for simple $k=0$ orthogonalized plane waves and for s functions meeting the Wigner-Seitz boundary condition. The points connected to the latter are Γ_1 levels obtained in the APW calculations. V_{muff} is the s-muffin-tin potential. With the exception of the spur marked Gr. Mult. all results were obtained in the average-of-configuration approximation. The spur (dot-dashed line) indicates results for the ground multiplets of Cr to Cu (ground-multiplet and average-of-configuration results are identical for Cu and Ni). The square boxes indicate APW, ground-multiplet potential, centers of gravity for comparison.

$$\Phi = (1-x)^{1/2}\Psi(d^n) + x^{1/2}\Psi(d^{n-1}s)\ . \qquad (12)$$

The s-potential difficulty encountered in connection with the first approach may be circumvented in the following approximate fashion. In the spirit of the Wigner-Seitz approximation one assumes that an electron must be present at the atomic site if it is to sample the potential at all. An s electron would then see only the second configuration in Eq. (12), the potential thus being

$$V_s(r) = (n-1)\chi_d(r)\ . \qquad (10c)$$

When $x \sim 0.75$, this potential will place the conduction bands ~ 0.5 eV lower with respect to a vacuum than Eq. (10b). Such a shift is not large compared with other uncertainties in the problem but is substantial in terms of the standards of accuracy set for band calculations.

This problem will be encountered in the present paper in connection with calculations involving a $d^n s^0$ configuration for which one cannot readily define an s potential. In the spirit of the Wigner-Seitz approximation, it will be assumed that the d electrons experience a $d^n s^0$ environment, while the s potential will be determined from a $d^{n-1}s^1$ configuration. [The s and d Coulomb contributions to the potential sampled by a d electron common to the two Ψ's of Eq. (12) are given by Eq. (10a).]

The preceding discussion is obviously incomplete, since it largely focuses on the difficulties encountered in the fractional occupancy situation without providing a satisfactory prescription for dealing with it. The relative sensitivity of ϵ_d and ϵ_Γ to the starting configuration chosen, which is exhibited in Fig. 4, emphasizes the fact that this problem deserves further attention.

III. RESULTS: ϵ_d AND ϵ_Γ

Figures 5 and 6 exhibit the values of ϵ_d and ϵ_Γ for $d^{n-1}s$ renormalized atoms for all $3d$ and $4d$ metals except Mn and Tc. As in the case of Fig. 3, these results were obtained by integrating re-

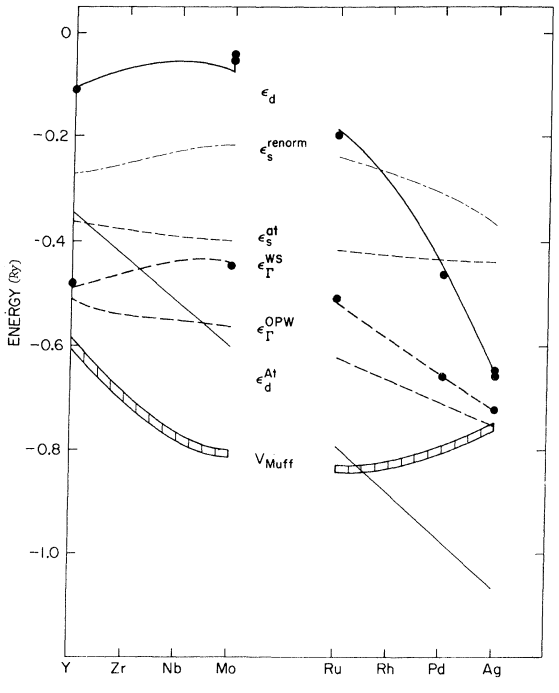

FIG. 6. Renormalized- and free-atom s and d one-electron energies for the $4d^{n-1}5s^1$ metals. Except for the lack of ground-multiplet data, these results are equivalent to those for the $3d$ metals in Fig. 5.

normalized $3d$ functions and both Wigner-Seitz s functions and simple $k=0$ OPW's in renormalized-atom d and s potentials over the Wigner-Seitz sphere. It is to be emphasized that the derived potential rather than one of the muffin-tin type is employed outside the APW radius. The shift of ϵ_d upon renormalization is again seen to reflect the behavior of the renormalization charge plotted in Fig. 2 which was discussed earlier.

APW band calculations have been performed for the metals having the structure underlined in Fig. 7. In order to compare the centers of gravity of the resulting d bands with ϵ_d it is best to consider suitable averages [e.g., $\frac{3}{5}\epsilon(\Gamma_{25'})+\frac{2}{5}\epsilon(\Gamma_{12})$] at high-symmetry points where hybridization is weak. These centers of gravity are shown as plotted points overlying the ϵ_d curves of Figs. 5 and 6. The agreement is seen to be excellent and confirms the physical and computational usefulness of ϵ_d in placing the d-band positions. Of course, the averages determining the center of gravity will depend slightly on the point in the Brillouin zone, e.g., Γ or X, chosen. The variation is illustrated in several cases by the two plotted points for a given element which are placed on the ϵ_d curve. The scatter is seen to be satisfyingly small and suggests that ϵ_d places the center of gravity of the d band about as well as the band calculations themselves.

Figures 5 and 6 also show several results associated with the conduction bands. These are the free-atom s level ϵ_s^{at}, the two estimates of ϵ_Γ, the s-potential muffin tins, and ϵ_s^{ren}. The latter correspond to the s levels calculated for the renormalized free-atom s function. These are of little use in placing either the bottom or some center of gravity of the conduction bands.

The s muffin-tin potential V_{muff} is seen to lie highest at the bottom of the d rows and to have a minimum near the middle. This behavior correlates with the lattice constant. The Wigner-Seitz radius is largest at the bottom of the d row and smallest near the middle. Such a correlation is to be expected because the muffin-tin region lies largely outside the core and d-electron charge. Accordingly, the potential in this region is essentially due to an effective singly positively charged ion core which contributes a $-2/R$ Coulomb potential. Here R is a characteristic radius for the muffin-tin region and is of the order of r_{WS}. From this estimate one finds indeed that V_{muff} follows, but lies lower than $-2/R$ across the rows by ~ 0.1 Ry. The discrepancy is due to exchange and to the fact that the inner part of the muffin-tin region penetrates some of the d charge. This latter effect is illustrated in Appendix A.

The placement of ϵ_Γ can be achieved as successfully as that of ϵ_d using the renormalized-atom viewpoint, provided the Wigner-Seitz method, where the energy is determined by requiring the wave function to be flat at r_{WS}, rather than an approximation based on a single OPW is used. The results of both calculations, labeled ϵ_Γ^{WS} and ϵ_Γ^{OPW}, are shown in Figs. 5 and 6. The band results are indicated by solid dots. These practically coincide with ϵ_Γ^{WS}, but, except for the elements at the extreme right of the rows, differ appreciably from ϵ_Γ^{OPW} and from V_{muff}. The single-OPW approximation[20] is evidently poor.

It should be noted that ϵ_Γ always lies above V_{muff}, the effect being largest in the middle of the row. Evidently the states between V_{muff} and ϵ_Γ are "non-propagating" and therefore forbidden to Bloch electrons.

The preceding discussion, particularly that concerning ϵ_Γ, has tacitly taken the band results as sufficiently reliable to serve as an absolute standard of comparison. This view may be somewhat misleading, since the standard APW procedure does not provide an exact representation of the eigenvalues and eigenfunctions of the full crystal potential and thus introduces errors of its own. It is thus particularly significant that the two methods of calculation are in substantially good agreement, and that the relatively simple renormalized-atom approach serves as a reliable means of placing the d and conduction bands relative to each other energetically. This relative placement has been a traditional source of difficulty in band calculations for the transition metals. The present $d^{n-1}s^1$ results, obtained with the renormalized-atom potentials, place the center of gravity of the d bands from zero to 1.5 eV higher, relative to ϵ_Γ, than do calculations[21] employing the standard superposition of $d^{n-1}s^1$ atomic charges plus full Slater exchange.

Sc	Ti	V	Cr	Mn	Fe	Co	Ni	Cu
HCP FCC	BCC (3.08) HCP FCC**	BCC (2.83)	BCC (2.69)	α FCC BCC*	BCC (2.67) FCC	HCP FCC (2.63)	FCC	FCC (2.67)
Y	Nb	Zr	Mo		Ru	Rh	Pd	Ag
HCP (3.77)	BCC	BCC HCP	BCC (2.93)		HCP (2.80)	FCC	FCC (2.88)	FCC (3.02)

* DISTORTED (i.e. BODY CENTERED TETRAGONAL)
** DOES NOT EXIST, HCP r_{WS} (=3.06) USED

FIG. 7. Crystal structures of the $3d$ and $4d$ metals. APW band calculations have been done for the cases underlined and the r_{WS} employed are in parentheses (in a.u.).

The results considered thus far have been obtained with potentials which average out spin multiplicity effects. Since these effects are of importance, particularly in materials like Cr, Fe, and Co having large paramagnetic moments, it is essential to obtain some measure of their effect. One might go about this by replacing the d contributions to the d potentials by those appropriate to the Hund's-rule ground multiplet of the $d^{n-x}s^x$ configurations in question. This view is oversimplified, but clearly something between it and the average-of-configuration description will be necessary to explain the magnetic properties of the transition metals.

Both the renormalized-atom prediction as well as the band results for ϵ_d using the ground-multiplet potential are shown in Fig. 5 for Cr and Fe. The results corresponding to the two descriptions are again seen to be in good agreement. However, the resulting ϵ_d lie significantly below their counterparts obtained from the average-of-configuration potential. The importance of acquiring an understanding and proper accounting of the metallic analog of Hund's rules for atoms if the d bands of the transition metals are to be placed accurately, i.e., to within some fraction of an eV, cannot be overemphasized.

The principal points made in this section, which are illustrated in Figs. 5 and 6, may be summarized as follows.

(i) The renormalized-atom energies ϵ_d and ϵ_Γ provide an excellent estimate of the energetic position of the center of gravity of the d band and conduction-band minimum, respectively.

(ii) ϵ_d is sensitive to the choice of the d-d exchange-correlation potential.

(iii) The renormalized-atom viewpoint is not successful in placing the bottom of the conduction band ϵ_Γ when the estimate is based on a single-OPW[20] rather than the Wigner-Seitz approach.

(iv) ϵ_Γ lies substantially above V_{muff} for most of the transition metals.

This latter point is of some importance in connection with Sec. IV, for most pseudopotential discussions of the transition metals have assumed $\epsilon_\Gamma = V_{muff}$ and use this to define a natural zero of the potential in the crystal, specifically, the level with respect to which d- and conduction-band positions are measured. V_{muff} will be chosen as the zero in Sec. IV. Different choices of course are possible, but they tend to worsen the numerical results.

IV. BAND WIDTHS, s-d HYBRIDIZATION, AND WAVE-FUNCTION CHARACTER

The Heine-Hubbard theory provides simple prescriptions for estimating the degree of d-conduction-band hybridization as well as d-band widths. This section implements these prescriptions using the renormalized-atom viewpoint. With some modifications, motivated by the Wigner-Seitz approach, the results obtained will be seen to be in satisfying agreement with those found from band calculations.

The strength of the d-conduction-band hybridization is determined by the parameter

$$\gamma = \int_0^{r_{WS}} j_2(\kappa r)\, V_d(r)\, P_d(r)\, r^2 dr \ . \tag{13}$$

Here j_2 is a spherical Bessel function, V_d is the d potential when zero is taken to coincide with V_{muff}, and

$$\kappa \equiv (\epsilon_d - V_{muff})^{1/2} \ . \tag{14}$$

The latter determines where the conduction band intercepts the resonant d levels. The definition of γ is the same as Hubbard's, but differs by a normalization factor from Heine's, Eq. (48a). It should be noted that γ is sensitive to the choice of κ since j_2 (and hence γ) is quadratic in κ for small κr. Furthermore, in the Heine-Hubbard and similar theories the product $P_d(r)V_d(r)$ is presumed to be small in the muffin-tin region. This assumption implies that contributions to the γ integration from the muffin-tin region are unimportant to the result. The present calculations which do not make the muffin-tin approximation indicate that the muffin-tin region makes approximately a 10% contribution to a computed γ.

The most visible measure of hybridization is the band gap along a given $\vec{k}$ direction which occurs where the conduction band intersects and mixes with the d bands. The gap and γ are linearly related. Heine reported crude estimates of γ values which correlated quite well with gaps obtained from band calculations. γ values for the various renormalized-atom d potentials have been obtained in the present work. The results are consistent[22] with Heine's observation, particularly if the κ of Eq. (13) is replaced by that at which the band gap actually occurs. Since the relation of γ to the s-d hybridization gap has been satisfactorily documented by Heine, no further quantitative comparisons will be made here.

The effects leading to s-d hybridization and intrinsic d-band width are almost inextricably woven together in the KKR or APW band formalisms. However, within the Heine-Hubbard scheme it is possible to separate the two effects, and, in particular, to estimate the d-band width quite simply. Heine suggested that the latter could be obtained by installing Wigner-Seitz boundary conditions corresponding to "bonding" and "antibonding" requirements that define the wave functions at the d-band minimum and maximum energy ϵ^{min} and ϵ^{max}, respectively. For the fcc, bcc, and hcp lattices these have been chosen to correspond to d states at points X, H, and M, in the respective Brillouin zones, for

which there is no s-d hybridization. Specifically, for the d functions $P(r)$ in question,

$$(dP/dr)_R = 0 \quad \text{when } \epsilon = \epsilon^{\min}, \tag{15a}$$

$$P(R) = 0 \quad \text{when } \epsilon = \epsilon^{\max}, \tag{15b}$$

R being the radius of a suitable sphere to be defined. The natural choice for R within a muffin-tin scheme is $R = r_{\mathrm{APW}}$. Then

$$P(R) = j_2(\kappa R) - \tan\eta_2\, n_2(\kappa R), \tag{16}$$

where

$$\tan\eta_2 = \kappa\gamma^2(\epsilon_d - \epsilon)^{-1} \tag{17}$$

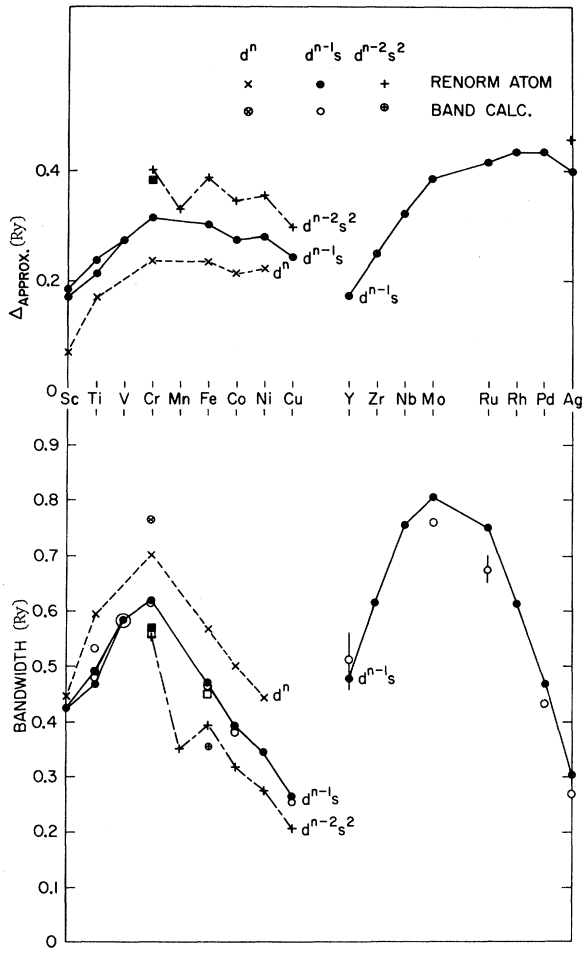

FIG. 8. d-band-width estimates for various $3d$ and $4d$ metal $d^{n-x}s^x$ configurations. The Δ_{approx}, at the top, were obtained with Heine's approximate expression [Eq. (19)]. The widths at the bottom were obtained by scaling Heine's complete expression [Eq. (18)] by 0.62 as is discussed in the text. The open circles or symbols enclosed by open circles are the results of APW band calculations. The open (APW) and filled [renormalized atom and Eq. (19)] squares are ground-multiplet results; otherwise all results were obtained in the average-of-configuration approximation.

is the phase shift associated with the d resonance. Equations (15) and (17) yield

$$\Delta \equiv \epsilon^{\max} - \epsilon^{\min} = \kappa\gamma^2\left(\frac{n_2'(\kappa R)}{j_2'(\kappa R)} - \frac{n_2(\kappa R)}{j_2(\kappa R)}\right). \tag{18}$$

Expanding the Bessel functions and their derivatives in the small-argument limit, one obtains

$$\Delta_{\mathrm{approx}} = 112.5\,\gamma^2/\kappa^4 R^5. \tag{19}$$

Heine employed this expression to estimate the band widths. Unfortunately, it differs from Δ of Eq. (18) by as much as a factor of 5 for the range of κR of interest here and thereby masks trends which might otherwise have been observable in Heine's data.

As stressed by Heine, there is some question as to the choice of R for which Δ should be evaluated. He made the plausible choice, $R = r_{\mathrm{APW}}$, meaning the boundary conditions are met halfway between nearest neighbors. The Δ_{approx}, for this choice, are plotted at the top of Fig. 8. The values of Δ obtained from Eq. (18) for the same choice are consistently larger than the APW band results. Scaled values 0.62Δ for the d-band widths are plotted at the bottom of Fig. 8 and compared to the results of band calculations. Leaving aside for the moment the rationale for scaling in this manner, one sees that with some scatter the scaled Δ track the band results very reasonably.

The band widths are largest for the d^n, where the d bands lie highest, and smallest for the $d^{n-2}s^2$ configurations, where they lie lowest. Because of the variation of κ, the errors in Eq. (19) vary significantly from one configuration to another and produce an inverted order of predicted band widths. The d-band widths obtained with the present $d^{n-1}s$ potentials are approximately the same for metals such as Cu and range up to almost 30% greater for Cr than the band widths obtained in band calculations[21] with potentials employing a superposition of atomic charges and the Slater exchange potential.

The necessity for scaling Δ disappears when it is recognized that Heine's choice of R was not ideal. A far better choice is $R = r_{\mathrm{WS}}$. This becomes clear from the results of Fig. 9, in which the d-band extrema are plotted and compared with the energies at which the d-electron $P(r)$ is noded and flat, respectively, at r_{WS}. The $P_d(r)$ determining the extrema were obtained in the spirit of the Wigner-Seitz approximation by integration in the full renormalized-atom $V_d(r)$ without utilizing the muffin-tin approximation. The agreement is extraordinarily good. The WS boundary conditions, applied at r_{WS}, are seen to determine the extrema of the d bands as deduced from an APW (or KKR) band calculation. The renormalized-atom viewpoint can thus be used to predict both the extrema as well as

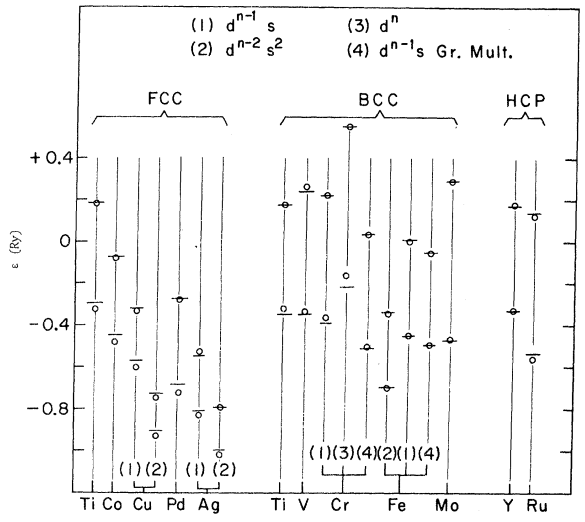

FIG. 9. Comparison of APW band results and the Wigner-Seitz boundary conditions. The lines indicate the extrema (X_3 and X_5 for fcc, H_{12} and H'_{25} for bcc, and first and tenth levels at M for hcp) of APW d bands employing l-dependent potentials inside the APW spheres and V_{muff} outside. The circles indicate the energies at which d functions (obtained by integrating in V_d throughout the full WS sphere) are flat (lower circles) and noded (upper circles) at r_{WS}.

the center of gravity ϵ_d of d bands.

Setting $R = r_{WS}$ leads to difficulties in the calculation of Δ from Eq. (18). These arise from problems surrounding the definition of κ. It no longer makes sense to employ V_{muff}, a potential inside r_{WS}, as the reference level in Eq. (14). The results of doing this, with $R = r_{WS}$ in Eq. (18), are inferior to the scaled results of Fig. 8. Replacing V_{muff} by the Γ_1-level position or by a potential such as $V_s(r_{WS})$ only improves matters moderately. While some variant of Eq. (14) might be defined so as to lead to Δ (for $R = r_{WS}$) values which are superior to the scaled result, it seems that the latter suffice, providing semiquantitative predictions and insight into the relation between band width and hybridization. In summary, it appears that quantitative predictions of d-band widths are best made by directly ascertaining the energies at which the Wigner-Seitz criteria are met.

Sample d-electron $P(r)$ for Co and Y are plotted[23] in Figs. 10 and 11, respectively, for various band energies. These are reminiscent of the results obtained by Wood[24] for Fe. The functions displayed correspond to energies ϵ_d and to the levels at X (for fcc Co) and M (for hcp Y) which were used as measures of the band width. The latter are seen to meet their respective Wigner-Seitz boundary conditions close to r_{WS}. The variation in Co wave-function character, from the bottom to top of the bands, is not severe because r_{WS} falls well out on the free-atom d-function tail. Renormalization effects are severest for Y (see Fig. 2) and consequently variation in $P(r)$ across the bands becomes greater, involving a factor-of-3 change in the charge residing in the inner wave-function loop. The renormalized free-$d^{n-1}s$-atom $P_d(r)$ are also plotted and are somewhat compressed with respect to the $P(r)$ obtained at ϵ_d. As we have already seen, these discrepancies have virtually no effect on renormalized-atom estimates of ϵ_d. The variation in band wave-function character and the discrepancies between it and the renormalized atom $P_d(r)$ are, however, of considerable interest to the question of self-consistent band potentials.

The Wigner-Seitz condition, applied at r_{WS}, has

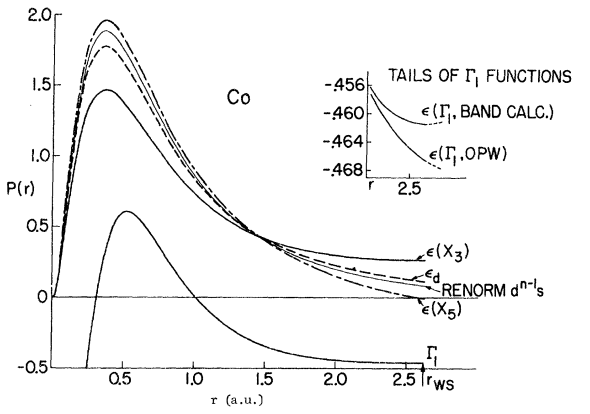

FIG. 10. Co radial fundtions $P_d(r)$ and $P_s(r)$ obtained by integration in renormalized-atom d and s potentials in the full Wigner-Seitz sphere. The d functions were obtained for energies at the bottom (X_3), top (X_5), and center of gravity (ϵ_d) of the bands. Also shown is the renormalized-free-atom d function appropriate to the d^8s configuration for which the band potentials were derived. Only the outer part (outside $r \sim 0.25$ a.u.) of $P_s(r)$, evaluated at the Γ_1-band energy, is shown in the figure and in the insert. The tail of the $P_s(r)$ obtained for the OPW estimated value of ϵ_Γ is also shown in the insert. Functions are normalized such that $\int_{WS} P(r)^2 r^2 dr = 1$.

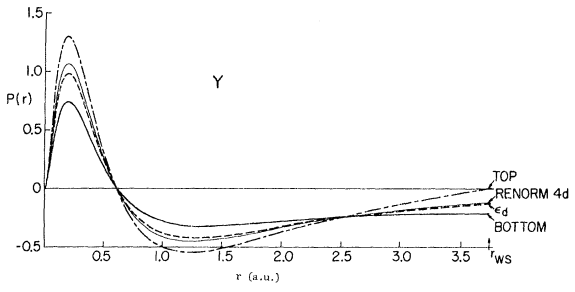

FIG. 11. Y radial function $P_d(r)$ obtained by integration in the renormalized d^2s V_d for the bottom, top, and center of gravity (ϵ_d) of the 4d bands. Also shown is the renormalized free-atom P_{4d} (r) for the same configuration.

been seen to determine the Γ_1 position of the conduction bands far more accurately than an estimate based on a single OPW. Our preliminary estimates[5] of renormalization effects were limited to Co, Ni, Cu, and Ag, for which we employed the single-OPW approximation. This works quite well, as can be seen in Figs. 5 and 6, and we did not realize the necessity for abandoning the OPW scheme until the metals in the middle of the transition-metal rows were considered. For these metals the Γ_1 wave function achieving the WS boundary condition is badly described by a single $k=0$ OPW, as will be seen below. The two functions are almost identical. While the Wigner-Seitz function is precisely flat at r_{WS}, the OPW used here is not.[20]

There is a qualitative difference between the ways the "bonding" d- and Γ_1 conduction-band states achieve the boundary conditions (15). As is illustrated in Figs. 10 and 11, the position R_0, where the d function is flat (after the final node), moves outward with increasing energy ϵ, i.e.,

$$dR_0/d\epsilon > 0 .$$

These considerations become more delicate when applied to s functions P_s at Γ_1, since these peak near r_{WS} rather than well inside as in the case of the d functions. In this case the wave-function "flat" in question therefore may correspond *either* to the tail of $P_s(r)$ as for the d functions *or* to the maximum of $P_s(r)$. For Cu and Ag, the $P_s(r)$ peak inside r_{WS} and the situation is the same as for the d bands; i.e., there is a condition on the wave-function tail,

$$dR_0/d\epsilon > 0 ,$$

with $R_0 = r_{WS}$. On the other hand, for the metals to the left of Ni and Pd the maximum of $P_s(r)$ would like to lie outside r_{WS}. Equation (15) then becomes a constraint requiring $P_s(r)$ to have its maximum at r_{WS} as is seen for Co in Fig. 10. In this situation a single $k=0$ OPW poorly represents the Γ_1 eigenfunction. Since the maximum of $P_s(r)$ moves inward with increasing energy, the preceding inequality is reversed, i.e., $dR_0/d\epsilon < 0$. This effect is most severe for Cr and Mo. Owing to rapidly increasing lattice constants, the effect diminishes as one moves from Cr and Mo to Sc and Y.

The boundary condition (15b) is of interest only in connection with the "antibonding" d states associated with the top of the band. As shown in Figs. 10 and 11, the position R_1 for which $P(R_1)=0$ moves inward with increasing ϵ. Thus $dR_1/d\epsilon < 0$. Heine's treatment of the d-band widths assumed $R_0 = R_1 = r_{APW}$. This assumption sets the d-band minimum too low and the maximum too high, thereby leading to too broad a band in relation to that obtained when $R_0 = R_1 = r_{WS}$.

The preceding considerations are of importance also if one wishes to examine, for example, the effects of pressure on various band states. The quantity of interest here is $d\epsilon/dr_{WS}$. Since $d\epsilon/dR_0 > 0$ and $d\epsilon/dR_1 < 0$, it is clear that compression of the lattice will produce d-band broadening when effects arising from any changes in potential are neglected. The variation of potential with pressure is expected to broaden the d bands further, and in addition to shift ϵ_d upward.

The position of Γ_1 will be similarly lowered under compression. However, the magnitude of the shift relative to the d-band edges is difficult to assess without recourse to detailed calculations. The present results show that, except in the vicinity of Cr and Mo, the shift in Γ_1 is smaller than that of the d-band minimum.

The discussion here has centered on wave functions, such as those plotted in Figs. 10 and 11, which result when the Schrödinger equation with the appropriate $V_s(r)$ or $V_d(r)$ is integrated outward to r_{WS} as is customary in the Wigner-Seitz method. This contrasts with the KKR (or APW) method, where one similarly employs the Schrödinger equation solution, at some ϵ and l, within the APW sphere and connects it to a wave function of the same l of the type displayed in Eq. (16). For κ defined by Eq. (14) and η_2 obtained from logarithmic derivatives at r_{APW}, the resulting muffin-tin-region wave functions are virtually identical to the results of direct integration in the renormalized-atom potential. The discrepancies are of the order of the width of the plotted lines in the figure. Good agreement is not surprising; boundary conditions fix the amplitude and slope of wave function (16) at r_{APW}, the function has approximately correct curvature, and the distance over which the function extends, i.e., r_{APW} to r_{WS}, is small. These results suggest that it is practicable to associate $l=2$ function of the type plotted in Figs. 10 and 11, which extends out to r_{WS}, to d-band eigenvalues obtained in a KKR or APW band calculation. This (and its extension to other l components of low-lying band states) has obvious computational implications. Calculations requiring band eigenfunctions become simplified and self-consistent band calculations employing renormalized-atom potentials become straightforward. A self-consistent treatment of the band potentials will yield d bands which lie somewhat lower and narrower than those reported here.

APPENDIX A: EXCHANGE

The purpose of this appendix is to extend the previous investigations of exchange potentials of Hartree[25] and Slater and collaborators,[26] and, in particular, to separate core-, d-, and "conduction"-electron effects. The problem with exchange

is, of course, its nonlocal character. The interaction potential can be rewritten as an effective local potential using a scheme originally employed[16] by the Hartree's. The local potential sampled by electron i becomes

$$V_{ex}^{i}(r)\,\phi_i(r) \equiv \Bigg(\sum_{\substack{\text{all occupied}\\ \text{states } j}} \delta(m_{s,i}, m_{s,j})\,\frac{\phi_j(r)}{\phi_i(r)} \times \int \phi_j^*(r')\,\phi_i(r')\,\frac{1}{|\vec{r}-\vec{r}'|}\,d^3r' \Bigg)\,\delta_i(r)\,, \tag{A1}$$

where the δ-function limits the interaction to electrons of like spin.

Three objections have been raised in the literature against the use of such exchange potentials in band calculations and hence in favor of approximations such as the local-density ($\rho^{1/3}$) type. These are as follows.

(a) That V_{ex}^{i} is strongly dependent on the spatial character of ϕ_i, not allowing a *single* given potential to be employed when integrating for eigenvalues and eigenstates throughout a band. This is thought to be particularly troublesome for d bands, for as Wood showed,[24] and we have seen here, there is considerable variation in radial character through a band.

(b) That the form of Eq. (A1) is sufficiently complicated that it is impracticable to use either in initial estimates of band potentials or in self-consistent band calculations. For the present purposes Eq. (A1) is to be integrated over a Wigner-Seitz cell and thus we require wave functions ϕ_i and ϕ_j defined in convenient form over the cell.

(c) That a $\rho^{1/3}$ potential is to be preferred as an approximation to a full *exchange-correlation* potential.

One conclusion of this appendix is that arguments (a) and (b) are not compelling while, for certain purposes, (c) may be. It is quite possible that electron-electron terms are best accounted for in free-electron bands by a $\rho^{1/3}$ local-density approximation. The results of the appendix, however, support the suggestion[1] that exchange contributions from ion cores be dealt with explicitly by Eq. (A1), perhaps with a polarization term to account for correlation effects. We also believe that a local-density approximation is neither necessary nor the most satisfying starting point for describing d-d exchange and correlation.

To set the discussion in perspective, let us inspect Fig. 1, which displays renormalized-atomic wave functions for Co d and s electrons as well as the $k=0$ OPW introduced earlier. The figure illustrates the extent to which d charge is concentrated inside and s- or conduction-electron charge outside one-half the Wigner-Seitz radius. The plotted s and d "regions" indicate the radii important to s- and d-electron energies and wave-function behavior and should be borne in mind when inspecting the exchange potentials in Figs. 12–16. (The variation in d character seen in Fig. 1 is suppressed because of renormalization, i.e., the free-ion Co^0 and Co^{++} d functions display greater variation and it is this greater variation which will be relevant here inasmuch as we are considering free-ion exchange potentials.)

Figure 12 displays the exchange potentials due to the argon core of a free Co^+ ion as sampled by a $4s$ electron and by $Co^0(d^9)$, $Co^+(d^8)$, and $Co^{++}(d^7)$ free-ion d functions. (V_{ex}^{4s} for the interior region, $r < 0.35$ a.u., has not been plotted.) This procedure was adopted in order to give some measure of how V_{ex} might vary with differing $3d$ radial character and hence how it might vary through a $3d$ band. Figure 13 similarly displays the exchange potential arising from the $3d^8$ shell of a Co^+ ion and Fig. 14 displays that arising from a single Co $4s$ electron. The sums of these terms, corre-

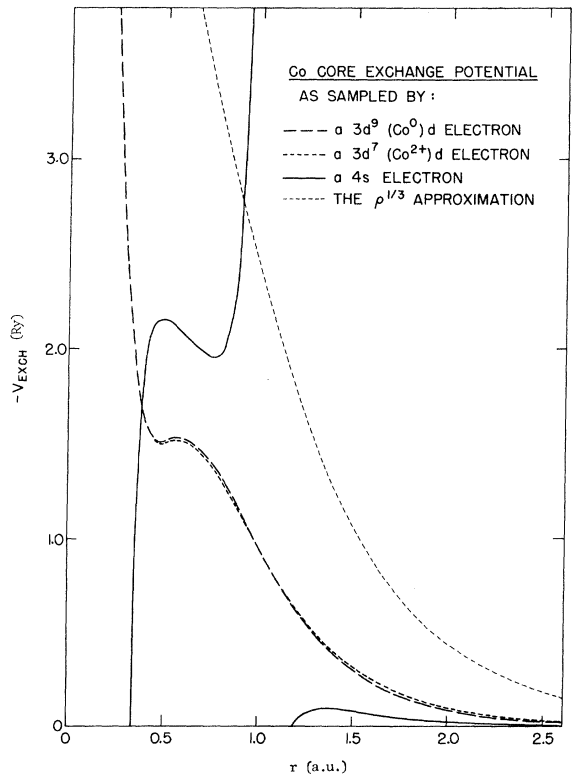

FIG. 12. Exchange potentials due to the argonlike core of a free Co^+ ion as sampled by a $4s$ orbital and by d orbitals appropriate to the $Co^0(d^9)$, $Co^+(d^8)$, and $Co^{+2}(d^7)$ ions. The $4s$ potential divergences arise owing to the $4s$ nodes which enter the denominator of Eq. (A1). The inner part of the $4s$ potential is not plotted. Also shown is the Slater $\rho^{1/3}$ approximation applied to the core charge density.

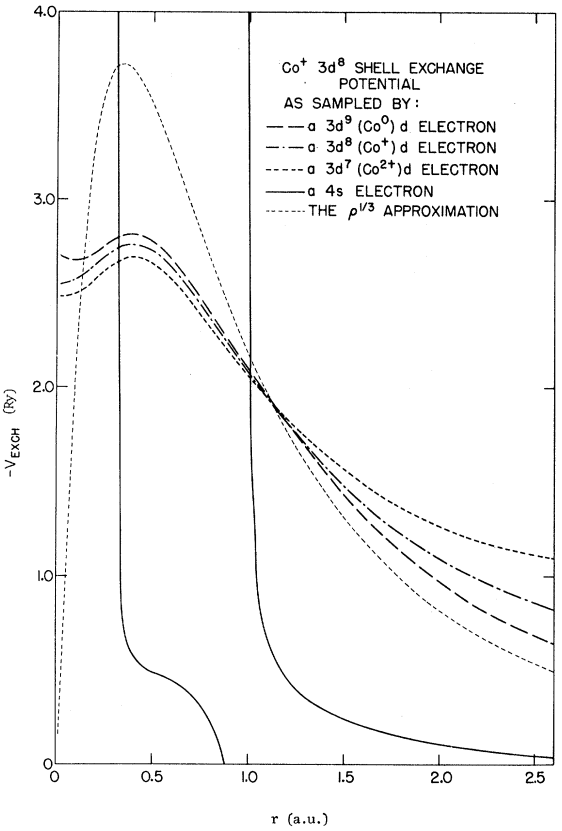

FIG. 13. Exchange potentials due to the $3d^8$ shell of a Co^+ ion as sampled by $4s$ and $3d$ orbitals in the manner of Fig. 12. The self-exchange d-d term is included in the d potentials. Also shown is the Slater $\rho^{1/3}$ approximation applied to the $3d$ charge density.

sponding roughly to a Co^0 $3d^8 4s$ atom, appear in Fig. 15. Also plotted in the figures are the $\rho^{1/3}$ evaluated in the Slater approximation,[11] with the densities of the particular electrons responsible for the exchange potentials in question. Since the contributions of various shells to a $\rho^{1/3}$ potential are not additive, it is not proper to make detailed quantitative comparison between the "partial" $\rho^{1/3}$ of Figs. 12–14 and the free-ion exchange potentials of Eq. (A1). Total ion $\rho_{tot}^{1/3}$ and exchange potentials were compared in the past,[26,27] as is proper. It is nevertheless valuable to consider core-, d-, and "conduction"-electron exchange contributions separately and it is perhaps also useful to have the partial $\rho^{1/3}$ for comparison.

Consider the core contributions to exchange shown in Fig. 12. Quite aside from the $4s$ divergences, the d and s potentials are quite different, but this poses no difficulty for APW or KKR band theory, which can easily incorporate l-dependent potentials inside the APW spheres, but less trivially outside, where the d potential is unimportant.

The $4s$ divergences arise from the nodes of ϕ_i in the denominator of Eq. (A1). The divergent regions are not important, since they are necessarily the regions where the $4s$ has little weight. We might note that in the outer region, important to a $4s$ electron, the partial $\rho^{1/3}$ term is larger than the exact exchange by almost an order of magnitude. Of greatest interest is the insensitivity of the d potential to d character. It should be recognized that wave-function *shape*, but not amplitude, is important to V_{ex} since ϕ_i's appear in numerator and denominator of Eq. (A1). In the case of the d electrons, appropriate to any given element, the wave functions have nearly fixed *shape* out through their maximum, no matter what their over-all behavior is. This fact tends to stabilize the exchange potential, making it relatively insensitive to the changes which occur in d ϕ_i in this region. Figure 12 suggests that fixed core-exchange potentials can be defined for either d or non-d bands and that any error introduced by not allowing for varying ϕ_i character is small compared with the other uncertainties in the problem. This encourages one to take seriously Hedin and Lundqvist's suggestion[1] that core-exchange effects be separated from conduction-electron–conduction-electron terms and treated rigorously.

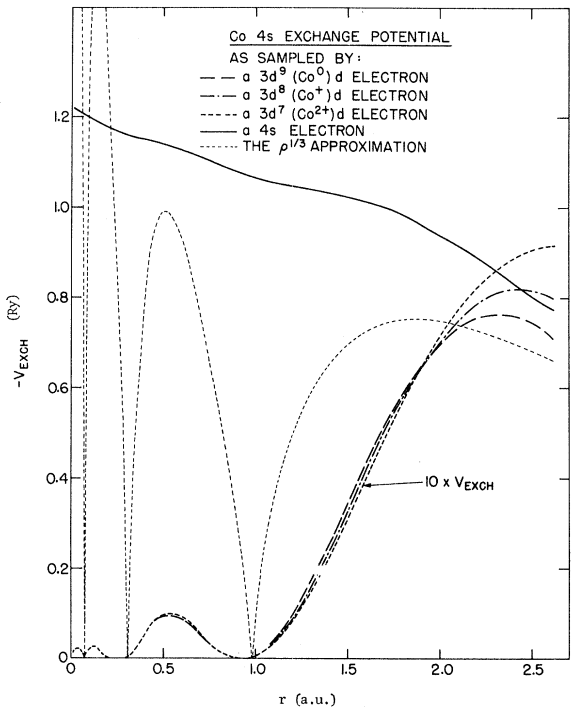

FIG. 14. $4s$-exchange-potential contribution as sampled by $4s$ and $3d$ orbitals in the manner of Fig. 12. The self-exchange s-s term is included in the $4s$ potential. Also included is the Slater $\rho_{4s}^{1/3}$.

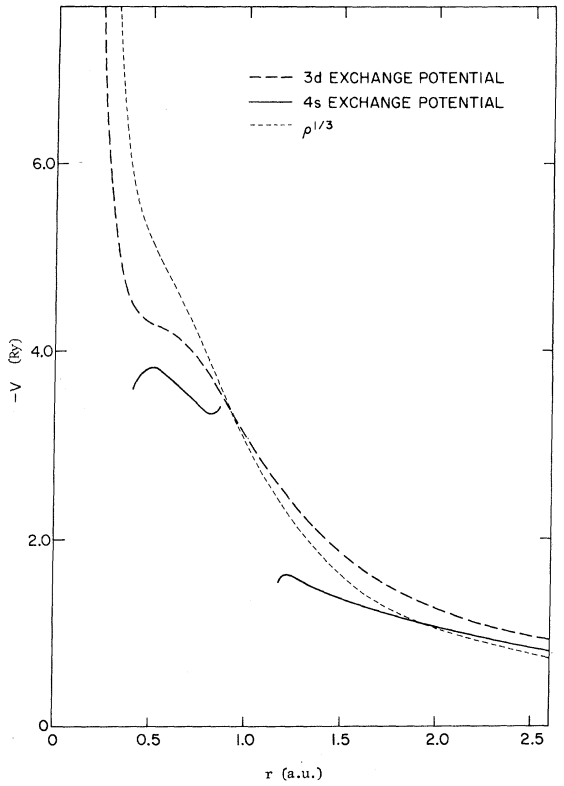

FIG. 15. Total exchange potentials, as sampled by $3d$ and $4s$ electrons due to the core, $3d$, and $4s$ shells of a $3d^8 4s$ Co atom. Also shown is the Slater $\rho^{1/3}$ approximation employing the full ion charge density.

The d-d exchange potentials of Fig. 13 include an intraelectronic self-exchange (or self-Coulomb) term unlike the core terms of Fig. 12, and as a result it is more appropriate to make comparisons between them and the partial $\rho_d^{1/3}$. Similarly, the s-s term of Fig. 14 is entirely a single self-exchange term. It provides the one case where an exchange term exceeds its partial $\rho^{1/3}$ counterpart and this fact is essential to the numerical agreement between the total $4s$ exchange potential and $\rho^{1/3}$ seen at larger r in Fig. 15. Again, more important is the insensitivity of the V_{ex}^d terms seen in Figs. 13 and 14, suggesting that it is not unreasonable to define a fixed total V_{ex}^d for purposes of a band calculation.

Figure 15 shows a now familiar result, namely, that the full Slater $\rho^{1/3}$ potential is in excellent agreement with the full $4s$ exchange potential in the outer regions of the atom important to $4s$ electrons and lies somewhat higher than the $3d$ potential in the $3d$ region. This result is reminiscent of Hedin and Lundqvist's treatment of the exchange problem.[1] They considered a local potential[11,12] of the form $\beta(\rho)\rho^{1/3}$, where β is a slowly varying local density-dependent amplitude, and utilized current electron-gas dielectric-function data to obtain the behavior of β appropriate to the *exchange-correlation* potentials for nearly-free-electron metals. β took on Slater's value in low-density regions and approached the $\frac{2}{3}$ value obtained by Kohn and Sham as density increased. Figures 12–14 suggest that the agreement of Fig. 15 depends on compensating cancellations in the different ways of calculating the exchange contributions and that a $\rho^{1/3}$ potential prescription which is satisfactory for the band calculation of a paramagnetic transition metal may run into difficulties in a "ferromagnetic" calculation employing different potentials for spin-up and -down bands. This is an interesting matter outside the scope of the present appendix.

It should be emphasized that when dealing with exchange effects in this paper we are assuming the Wigner-Seitz approximation, with its full self-Coulomb hole at the Wigner-Seitz cell in question. This is an assumption concerning correlation effects. The situation is at least superficially similar to Hartree-Fock theory for a free atom where an occupied one-electron state has a full Coulomb hole attached to the atomic site, but it is quite different from a straight Hartree-Fock derivation for bands in a solid. Consider the one-center exchange

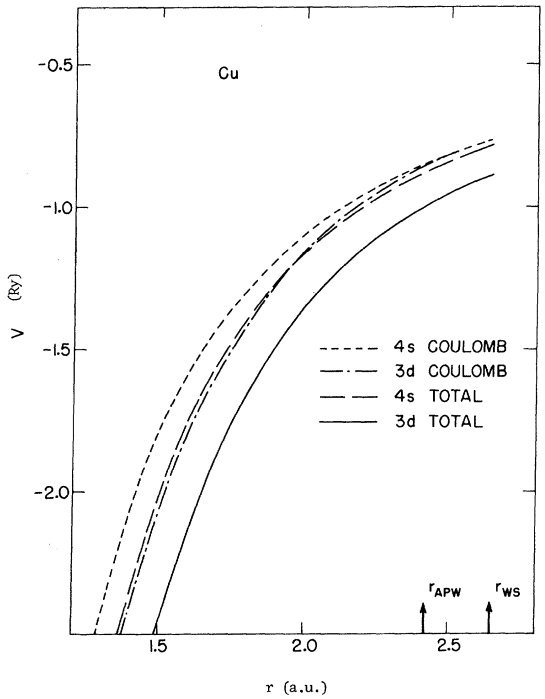

FIG. 16. Outer regions of renormalized Cu $d^{10}s$ atom Coulomb and total potentials as sampled by $3d$ and $4s$ electrons. The Coulomb potentials include the self-exchange or Coulomb-hole terms. The total potential includes the additional interelectronic exchange terms in the average-of-configuration approximation.

terms associated with a tight-binding description of a band. It may be shown that the resulting one-center self-exchange-like term is proportional to the fractional occupation of that band. Since a single-center integral of this type is of the order of 1–2 Ry, its effects on the band results are very large indeed. For extreme population differences, it might shift one band level with respect to another by as much as 10 eV from the levels predicted with $\rho^{1/3}$ or renormalized-atom potentials. The correlation assumptions associated with the renormalized-atom description may be incomplete but they are more satisfying than a literal Hartree-Fock derivation whose effective self-Coulomb hole depends on the accident of band occupation and on the nature of multicenter exchange terms.

One final matter deserves attention before concluding this appendix. In the course of constructing separate d and non-d potentials for various transition metals, we noted that the d potential invariably lay deeper in the outer portions of the cell. One might assume that this is due to better screening of the nucleus by d electrons, since they are concentrated nearer the nucleus. Figure 16 shows this argument to be incorrect. The "Coulomb" terms include the subtraction of the self-Coulomb or exchange hole; i.e., a d-electron experiences a $d^{n-1}s^x$ Coulomb potential and an s a $d^n s^{x-1}$ potential. We see that the two terms, thus defined, are essentially identical in the muffin-tin region and that the entire discrepancy in total potentials is due to *inter*-electronic exchange effects. In other words, a conduction electron is almost as effective as a d in Coulomb screening of the outer part of a Wigner-Seitz cell. Even though the d potential in this region is not of great quantitative importance to d-band behavior, the result serves to underscore the importance of improving the understanding of exchange-correlation effects in such problems as those of concern in the main part of this paper.

In conclusion, the experience with Figs. 12–14 suggests that fixed d and non-d exchange potentials can be satisfactorily used in band calculations providing they are taken to be different and that the error in doing this is slight compared with the other uncertainties in the problem. The explicit introduction of exchange can be readily accomplished with the renormalized-atom approach, but not when free-atom charge densities are standardly superposed. In addition, the latter approach violates the Pauli exclusion principle in its description of Coulomb terms. Given d and non-d wave-function components defined over the full Wigner-Seitz cell, it should be possible to construct self-consistent band potentials with exchange treated directly. It is our intention to return to this matter in a later paper. The important criterion in the choice between a local-density-dependent potential and one in the family of Eq. (A1) is a matter of physical insight. A $\rho^{1/3}$ approximation may be preferable for conduction-electron–conduction-electron effects, though this has not been used in this paper. Core contributions are possibly best treated within the exchange approximation, perhaps with polarization terms.[1] We consider the explicit treatment of exchange to be both practicable and better than the $\rho^{1/3}$ approximation when dealing with intra-atomic d-d exchange and correlation in a metal.

APPENDIX B: CALCULATIONS

When available, analytic Hartree-Fock wave functions[27] were used as the starting point of the renormalized-atom calculations. Such functions were, in general, not available for the $d^{n-1}s^1$ configuration. For this configuration the d and s Hartree-Fock equations were solved to self-consistency, numerically. Exchange and Coulomb terms due to fixed Ar- or Kr-like cores, of the +1-charged d^{n-1} ions, were employed. These free-atom functions, the renormalized functions, and resulting potentials were generated on the Herman-Skillman radial mesh[28]; i.e. renormalization was to the mesh point closest to the crystalline r_{WS}.[29] This introduced only slight errors, since the Herman-Skillman mesh is reasonably fine in the vicinity of the r_{WS}.

The band calculations were performed employing the APW-energy-band programs available at Iowa State University. The APW energy bands were calculated using the $l=2$ logarithmic derivatives obtained using the V_d potential and logarithmic derivatives for other l, from 0 to 12, obtained using the V_s potential. This was sufficient for our purposes, though one might be tempted to employ more V_l. Segall used a V_s, V_p, and V_d in his calculation[10] for Cu. We were not prepared to deal with an l-dependent muffin-tin region and therefore used the s muffin tin V_{muff}. This choice was dictated by the fact that the muffin-tin region is important to the conduction but not to the d-electron energy levels. V_{muff} tends to lie something like 0.1 Ry higher than its d counterpart, as is suggested by Fig. 16, thus raising d energies. The states at the bottom of the d bands are most diffuse (see Figs. 10 and 11) and hence are most affected. Their energies may be as much as 0.03 Ry higher than they would be for a pure d potential. Energies in the bulk of the d bands, and the ϵ_d, are affected by less than 0.01 Ry.

APPENDIX C: LATTICE CONTRIBUTIONS TO SPHERICAL POTENTIAL

In first approximation, the spherical potential inside a neutrally charged Wigner-Seitz cell arises from the charge within that cell. This could be modified somewhat if the exchange-correlation hole were permitted to wander outside the cell,

but at least the spherical Coulomb potential comes predominantly from the charge inside. There are additional small multipole contributions arising from the fact that the charge outside is not spherically distributed about the cell in question. The renormalized-atom approach is particularly convenient if such contributions can be ignored. The purpose of this appendix is to determine their importance in fcc and bcc lattices. We will see that these multipole effects shift the potential by $\sim 2\times10^{-5}$ Ry or less and hence are insignificant.

We will follow Rose's expansion[30] for the interaction of some charge distribution $\rho(\vec{r}')$ in a central region, with a distribution $\rho_i(\vec{r})$ in some region $\vec{R}_i$ away, $\vec{r}'$ and $\vec{r}$ being defined from the end points of $\vec{R}_i$. The particular expansion only holds[31] if $R_i > r + r'$ (i.e., it will not yield a proper definition of the potential in the outermost region of the Wigner-Seitz cell due to charge in the outermost part of a nearest-neighbor WS cell) but it will suffice for our purposes here. The spherical potential obtained in the central region is a constant of the form

$$V_{\text{spher}} = 8\pi \sum_i \sum_{m,L} \frac{(-)^L}{2L+1} [(2L)!]^{-1/2} \times \frac{1}{R_i^{L+1}} Y_L^m(\hat{R}_i) M_L^{-m}(i) , \quad \text{(C1)}$$

where the moment

$$M_L^m(i) \equiv \int_{\text{region } i} \rho(\vec{r}) r^L Y_L^m(\hat{r}) d\tau . \quad \text{(C2)}$$

The leading term for a cubic lattice has $L = 4$, $m = 0$, and we will limit consideration to this. There will, in general, be two contributions to the M_4^0, the first from any asphericity in the d-electron charge and the second from the fact that the Wigner-Seitz cells are not spherical. The latter dominates since the net deviation from d-band sphericity generally involves a few tenths of a cubic d electron's charge *and* because $\langle r^4 \rangle$ tends to be much smaller than r_{WS}^4, a value characteristic of the second term. Assuming a constant charge density ρ in the contributing muffin-tin region, the second term,

$$M_4^0 = (5/4\pi)^{1/2} \rho \int r^4 P_4^0(\cos\theta) d\tau , \quad \text{(C3)}$$

where the integral extends over the muffin-tin region, takes on the numerical values 155 and 145 a.u. for Cu in a fcc and bcc WS cell, respectively, and 1710 and 1580 a.u. for Y in a fcc and bcc WS cell, respectively.

The Cu and Y lattices are among the smallest and largest encountered in the $3d$ and $4d$ metals. Hence their r_{WS} provide bounds on what can be expected from the above term. The lattice sum of Eq. (C1) has been carried out to ninth neighbors in the fcc and to but second neighbors in the bcc lattice. The smaller summation suffices for our purposes and with typical muffin-tin-region charge densities of 0.01–0.03 electrons per a.u.^{3} one obtains $V_{\text{spher}} \sim -2\times10^{-5}$ Ry for the r_{WS} corresponding to Y at the larger density in either the fcc or bcc lattice. About half this value is obtained for the Cu lattice. Contributions from d asphericity are something like an order of magnitude smaller.

We thus arrive at the expected result that the external multipole contributions to the spherical potential are unimportant; only the central-cell terms are significant.

---

*Work supported by the U. S. Atomic Energy Commission.

†Work supported in part by Grant No. GP-16504 of the National Science Foundation and the Advanced Research Projects Agency.

[1]E.g., see L. Hedin and S. Lundqvist, Solid State Phys. 23, 2 (1969).

[2]J. H. Van Vleck, Rev. Mod. Phys. 25, 220 (1953).

[3]J. Hubbard, Proc. Roy. Soc. (London) A276, 238 (1963); A277, 237 (1964); A281, 401 (1964).

[4]M. C. Gutzwiller, Phys. Rev. Letters 10, 159 (1963); Phys. Rev. 134, A923 (1964); see also J. Kanamori, Progr. Theoret. Phys. (Kyoto) 30, 275 (1963); C. Herring, in *Magnetism*, edited by G. T. Rado and H. Suhl (Academic, New York, 1966), Vol. IV.

[5]R. E. Watson, H. Ehrenreich, and L. Hodges, Phys. Rev. Letters 24, 829 (1970), in which preliminary results of the present work are given.

[6]V. Heine, Phys. Rev. 153, 673 (1967).

[7]J. Hubbard, Proc. Phys. Soc. (London) 92, 921 (1967); J. Hubbard and N. W. Dalton, J. Phys. C 1, 1637 (1968); J. Hubbard, *ibid.* 2, 1222 (1969).

[8]R. L. Jacobs, J. Phys. C 1, 492 (1968).

[9]M. Chodorow, Phys. Rev. 55, 675 (1939).

[10]B. Segall, Phys. Rev. 125, 109 (1962).

[11]J. C. Slater, Phys. Rev. 81, 385 (1951).

[12]R. Gaspar, Acta Phys. Hung. 3, 263 (1954); P. Hohenberg and W. Kohn, Phys. Rev. 136, B864 (1964); W. Kohn and L. J. Sham, *ibid.* 140, A1133 (1965); L. J. Sham and W. Kohn, *ibid.* 145, 561 (1966).

[13]E.g., R. E. Watson and H. Ehrenreich, Comments Solid State Phys. 3, 109 (1970).

[14]K. Levin and H. Ehrenreich, Phys. Rev. B 3, 4172 (1971); R. E. Watson, J. Hudis, and M. L. Perlman, *ibid.* 4, 4139 (1971).

[15]H. Brooks, Nuovo Cimento Suppl. 7, 165 (1958); or P. W. Anderson, *Concepts in Solids* (Benjamin, New York, 1964).

[16]D. R. Hartree, *The Calculation of Atomic Structures* (Wiley, New York, 1957).

[17]G. H. Shortley, Phys. Rev. 50, 1072 (1936); J. C. Slater, *Quantum Theory of Atomic Structure* (McGraw-Hill, New York, 1960), Vol. I, Chap. 14.

[18]E.g., see J. C. Slater, J. B. Mann, T. M. Wilson, and J. H. Wood, Phys. Rev. 184, 672 (1969).

[19]We should note that the average of configuration

scheme has only been rigorously derived for integral electron count and application to fractional count does not consider the problem raised here.

[20]The OPW employed here involves orthogonalization to a single site. C. Herring [Phys. Rev. 57, 1169 (1940)] has pointed out that the single-site approximation is incorrect when one has as large ion cores, relative to r_{WS}, as we appear to have here.

[21]E. C. Snow and J. T. Waber, Acta Met. 17, 623 (1969).

[22]The band gaps typically occur about halfway out from point Γ to the Brillouin-zone boundary. Some measure of how well γ describes hybridization at other k can be obtained by comparison with the hybridization parameters employed by L. Hodges [Ph.D. thesis (Harvard University, 1966) (unpublished)], L. Hodges, H. Ehrenreich, and N. D. Lang [Phys. Rev. 152, 505 (1966)], and H. Ehrenreich and L. Hodges [Methods Comput. Phys. 8, 149 (1968)] and by F. M. Mueller [Phys. Rev. 153, 659 (1967)] in their interpolation schemes, where their parameters are determined by band-calculation results. It appears that their parameters very crudely agree with the calculated γ but γ lies somewhat higher near the zone boundaries. Discrepancies in this region are serious inasmuch as hybridization is strongest at large k; γ is roughly proportional (Ref. 6) to κ^2 over the full range of κ, whereas the band parameters have flattened out at the zone boundary. The reason why the parameters do not track γ in detail is not understood. It should be noted that neither the γ of Eq. (13) nor the interpolation-scheme parameters explicitly include terms arising from the nonorthogonality between the d and continuum states (see Hodges's thesis). A correction for this is not expected to substantially improve agreement between the two, for the correction to γ will have its κ dependence largely residing in an overlap integral, which, like the term it is correcting, is proportional to κ^2; thus $\gamma(\kappa)$ is expected to remain roughly proportional to κ^2.

[23]Unlike Fig. 1, $P(r)$ rather than $rP(r)$ is considered here. These plots display the outside boundary conditions more directly, although they provide less sense of where the charge density resides.

[24]J. H. Wood, Phys. Rev. 126, 517 (1962).

[25]D. R. Hartree, Phys. Rev. 109, 840 (1958).

[26]J. C. Slater, T. M. Wilson, and J. H. Wood, Phys. Rev. 179, 28 (1969).

[27]R. E. Watson, Phys. Rev. 118, 1036 (1960); 119, 1934 (1960); R. E. Watson and A. J. Freeman (unpublished).

[28]See F. Herman and S. Skillman, *Atomic Structure Calculations* (Prentice-Hall, Englewood Cliffs, N. J., 1963).

[29]See Fig. 7 for the crystalline r_{WS} employed for the cases for which band calculations were done.

[30]M. E. Rose, J. Math & Phys. 37, 215 (1958).

[31]R. J. Buehler and J. O. Hirschfelder, Phys. Rev. 83, 628 (1951).